

1 Article

2 Photocatalytic Degradation of Azo Dye Reactive 3 Violet 5 on Fe-Doped Titania Catalysts under Visible 4 Light Irradiation

5 Antonio Zuorro ^{*,1}, Roberto Lavecchia ¹, Marika Michela Monaco ¹, Giuseppina Iervolino ²,
6 Vincenzo Vaiano ²

7 ¹ Department of Chemical Engineering, Materials and Environment, Sapienza University, 00184 Rome, Italy;
8 antonio.zuorro@uniroma1.it (A.Z.); roberto.lavecchia@uniroma1.it (R.L.);
9 marikamichela.monaco@uniroma1.it (M.M.M.)

10 ² Department of Industrial Engineering, University of Salerno; giervolino@unisa.it (G.I.); vvaiano@unisa.it
11 (V.V.)

12 * Correspondence: antonio.zuorro@uniroma1.it

13 Received: date; Accepted: date; Published: date

14 **Abstract:** The presence of azo dyes in textile effluents is an issue of major concern due to their
15 potential impact on the environment and human health. In this study we investigate the
16 photocatalytic degradation under visible light of Reactive Violet 5 (RV5), an azo dye widely used in
17 the textile industry. A preliminary screening of different titania-based catalysts was carried out to
18 identify the best candidate for RV5 removal. The selected catalyst was then tested in a stirred and
19 aerated lab-scale reactor illuminated with a light LED source ($\lambda_{\max} = 460$ nm). The effects of pH,
20 catalyst load and hydrogen peroxide additions on the efficiency of dye removal were evaluated.
21 Under the best conditions (pH 10, 3 g/L of catalyst and 60 mM hydrogen peroxide), the dye
22 solution was completely decolorized in about 2 h. Overall, the results obtained suggest that the
23 proposed process may represent a suitable method for the removal of RV5 from textile effluents.

24 **Keywords:** photocatalysis; visible light; titania catalysts; azo dye; reactive violet 5; textile
25 wastewater

27 1. Introduction

28 Azo dyes are the largest class of dyes used in industry [1]. These compounds are characterized
29 by the presence of one or more azo bonds ($-N=N-$) in their molecule in association with one or more
30 aromatic structures [2]. In the textile industry, the use of azo dyes for coloring cellulosic fibers such
31 as cotton and wool has increased significantly over the last decades due to their cost effectiveness,
32 brightness of color and good resistance to washing and light exposure. A major drawback related to
33 their application on textiles is the low fixation yield of the dye on the fiber caused by the hydrolysis
34 of the reactive groups in the dye molecule [3]. As a result, up to about 30% of the initial amount of
35 dye can be lost in water [4].

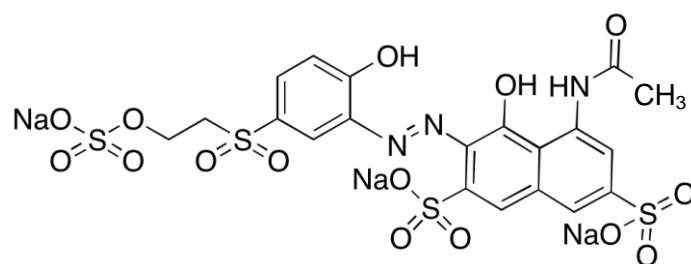
36 The presence of azo dyes in textile effluents makes them particularly harmful to the
37 environment and to human health [5]. In fact, their release into aquatic ecosystems may lead to a
38 reduction of sunlight penetration and dissolved oxygen concentration, with deleterious effects on
39 local flora and fauna [6]. In addition, toxic and potentially carcinogenic compounds such as aromatic
40 amines can be formed during dye degradation [7]. For these reasons, textile wastewater needs to be
41 properly treated.

42 Since conventional water treatments are often ineffective in eliminating azo dyes from textile
43 effluents, more efficient technologies, such as the advanced oxidation processes (AOPs), are used
44 [8,9]. AOPs are based on the generation of highly reactive radical species, such as hydroxyl radicals

45 ($\cdot\text{OH}$), by solar, chemical or other forms of energy. These radicals can attack the target compounds
46 through different reaction mechanisms leading to their degradation [10, 11].

47 In this paper we investigate the degradation of Reactive Violet 5 (RV5) by a photocatalytic
48 treatment with Fe-doped TiO_2 photocatalysts exposed to visible light. RV5 is widely used in textile
49 dyeing because of its brightness, ease of application and good fastness to washing. However, its
50 complex aromatic structure (Figure 1) makes it highly resistant to degradation. A literature survey
51 shows that very few studies have been performed on RV5 degradation, and none of them has
52 investigated the photocatalytic removal of the dye under visible light [12–16]. Accordingly, a first
53 aim of this study was to evaluate whether the use of the selected photocatalyst in the presence of
54 visible light could be a suitable method to degrade RV5. Second, we were interested in assessing the
55 effect of the main process parameters on the efficiency of dye removal and the possibility of
56 enhancing it by addition of hydrogen peroxide.

57 The results obtained indicate that the proposed process may represent a viable and promising
58 approach for the removal of RV5 from textile effluents.



68 **Figure 1.** Chemical structure of azo dye Reactive Violet 5 (RV5).

69 2. Materials and Methods

70 2.1. Materials

71 Sodium hydroxide (NaOH , CAS 1310-73-2), sodium hydrogen carbonate (NaHCO_3 , CAS
72 144-55-8), disodium hydrogen phosphate (Na_2HPO_4 , CAS 7558-79-4), potassium dihydrogen
73 phosphate (KH_2PO_4 , CAS 7778-77-0), sodium acetate (CH_3COONa , CAS 127-09-3), acetic acid
74 (CH_3COOH , CAS 64-19-7) and hydrogen peroxide (30 wt% in water, CAS 7722-84-1), iron
75 acetylacetonate ($\text{Fe}(\text{C}_5\text{H}_7\text{O}_2)_3$, CAS 14024-18-1), titanium isopropoxide ($\text{C}_{12}\text{H}_{28}\text{O}_4\text{Ti}$, CAS 546-68-9)
76 were purchased from Sigma-Aldrich Co. (St. Louis, Mo, USA). All chemicals were reagent grade and
77 used as received.

78 RV5 of technical grade ($\text{C}_{20}\text{H}_{16}\text{N}_3\text{Na}_3\text{O}_{15}\text{S}_4$, MW 735.59 g mol^{-1} , color index number 18097) was
79 provided by Gammacolor Srl (Seveso, Italy) and used as received. The natural pH of the dye
80 solution was 7.2 ± 0.1 . When needed, RV5 was dissolved in the following buffers: acetate buffer (0.1
81 M, pH 4), phosphate buffer (0.1 M, pH 6 and 8) and carbonate buffer (0.1 M, pH 10 and 12).

82 2.2. Catalysts Preparation and Characterization

83 P-25 Degussa was obtained from Sigma-Aldrich Co. (St. Louis, Mo, USA). Fe- TiO_2
84 photocatalysts were prepared by sol-gel method. In particular, 50 mg of iron acetylacetonate was
85 dissolved in 25 mL of titanium isopropoxide. The obtained solution was sonicated in order to obtain
86 the complete solubilization of iron acetylacetonate. Then, 100 mL of distilled water were added to
87 obtain a precipitate which was separated from the liquid phase by centrifugation for 5 min at 5,000
88 rpm. The sample was washed with distilled water for three times to remove any impurities and it
89 was calcined at 450°C for 30 min [17]. The obtained samples were named $x\text{Fe-TiO}_2$ where x is the
90 amount (in mg) of iron acetylacetonate used in the synthesis. The list of the prepared photocatalysts
91 with the amount of chemicals used in the preparation procedure is reported in Table 1.

92 All the photocatalysts were characterized using different techniques. The Raman spectra of the
 93 samples were recorded with a Dispersive MicroRaman system (Invia, Renishaw), equipped with 514
 94 nm laser, in the range 100-2,000 cm^{-1} Raman shift. The crystal phases of photocatalysts were
 95 determined by XRD analysis carried out on Bruker D8 diffractometer, using $\text{Cu-K}\alpha$ radiation. The
 96 surface area (SSA) of the catalysts was obtained from the dynamic N_2 adsorption measurement at
 97 -196°C , using a Costech Sorptometer 1042 instrument, after a pre-treatment of the samples at 150°C
 98 for 30 min in He flow. UV-vis reflectance spectra of powder catalysts were recorded by a Perkin
 99 Elmer spectrometer Lambda 35 using an RSA-PE-20 reflectance spectroscopy accessory (Labsphere
 100 Inc., North Sutton, NH). All spectra were obtained using an 8° sample positioning holder, giving
 101 total reflectance relative to a calibrated standard SRS-010-99 (Labsphere Inc., North Sutton, NH).
 102 Equivalent band gap determinations of the photocatalysts were obtained from Kubelka-Munk
 103 function $F(R_\infty)$ by plotting $[F(R_\infty) \times hv]^2$ vs. hv .

104 **Table 1.** List of the prepared photocatalyst, amount of chemicals used in the synthesis and Fe/Ti
 105 molar ratio.

Photocatalysts	$\text{Fe}(\text{C}_5\text{H}_7\text{O}_2)_3$ Amount [mg]	Titanium isopropoxide [mL]	Distilled water [mL]	Fe/Ti molar ratio [mol/mol]
TiO_2	0	25	100	0
10Fe- TiO_2	10	25	100	0.00033
50Fe- TiO_2	50	25	100	0.0017
100Fe- TiO_2	100	25	100	0.0033

106 2.3. Photocatalytic Apparatus

107 The experimental apparatus consisted of a borosilicate glass cylindrical photoreactor (ID = 3 cm,
 108 H = 18 cm) equipped with an air distributor and a magnetic bar. A flexible LED strip (SMD 5050, 60
 109 LED/m, 0.24 W/LED) with an overall length of 1.5 m was wrapped around the reactor and used as
 110 light source. The emission wavelength of the LEDs was 460 nm. The air distributor provided a
 111 maximum flow rate of 300 NL/h and was placed at the bottom of the reactor, just above the stirring
 112 bar. Darkness conditions were achieved by covering the photocatalytic apparatus with an aluminum
 113 foil.

114 2.4. Photodegradation Experiments

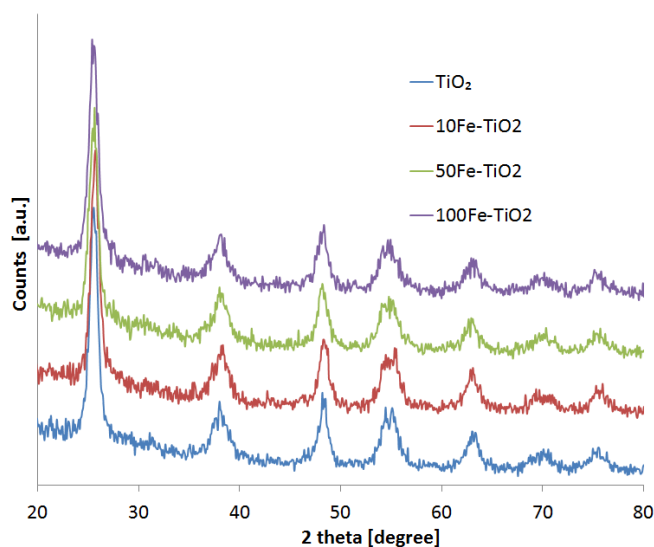
115 Photodegradation experiments were carried out by putting 50 mL of the aqueous solution
 116 containing the dye and the catalyst in the reactor. The system was left in the dark under stirring for 1
 117 h to allow the adsorption-desorption equilibrium of RV5 on photocatalyst surface. Then, the light
 118 source was switched on and the reactor was aerated. At the desired time, a small sample of liquid
 119 was taken, filtered at $0.45\ \mu\text{m}$ and analysed spectrophotometrically. Measurements were made on a
 120 double-beam UV-Vis spectrophotometer (UV-2700, Shimadzu, Japan) at 560 nm, where the
 121 absorption spectrum of RV5 displays a maximum. The stirring rate was set at 400 rpm and the air
 122 flow rate at 200 NL/h. The initial dye concentration was varied between 20 and 100 ppm and the
 123 catalyst load between 0.5 and 6 g/L. When required, hydrogen peroxide was added in the
 124 appropriate amount to the reaction mixture.

125 3. Results and Discussion

126 3.1. Catalysts characterizations

127 The XRD results of undoped and doped TiO_2 with different Fe content are reported in Figure 2 It
 128 was possible to observe that the crystalline structure of the photocatalysts showed only patterns
 129 related to anatase TiO_2 for all the samples [18]. No signals due to iron oxides appear in the XRD
 130 patterns, suggesting insignificant iron segregation in Fe-doped TiO_2 samples [19].

131



132

133

Figure 2. XRD spectra of the photocatalysts.

134

135

136

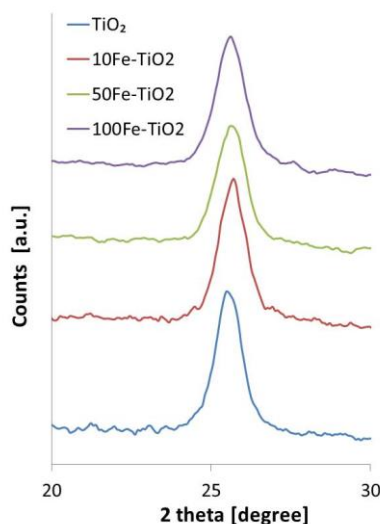
137

138

139

140

Since the ionic radius of the Fe³⁺ ion (0.064 nm) is smaller than that one of the Ti⁴⁺ ion (0.068 nm) [20], and considering that the Pauling electronegativities of Fe³⁺ (1.83) and Ti⁴⁺ (1.54) are similar [21], Fe³⁺ ions may enter the crystal cell of TiO₂ at substitutional sites [22]. To better investigate this aspect, the XRD spectra of the photocatalysts were more accurately analyzed in the range 20–30° (Figure 3).



141

142

Figure 3. XRD spectra of the photocatalysts in the range 20–30°.

143

144

145

146

147

148

149

150

151

It is possible to observe that the diffraction peak of undoped TiO₂ at about 25.3° shifted to higher angle for all the Fe-doped TiO₂ samples, indicating that doping of TiO₂ with iron led to a decrease of the lattice parameters. This phenomenon is a clear indication that our preparation method for the doped photocatalysts induced a replacement of the lattice Ti⁴⁺ ions by Fe³⁺ ions [22], evidencing, therefore, the successful doping of the TiO₂ crystalline structure with iron.

The crystalline size of the photocatalysts was calculated on the diffraction pattern visualized in Figure 3, using Scherrer's formula (Table 2).

152

Table 2. List of the prepared photocatalyst and their characteristics.

Photocatalysts	Crystalline size [nm]	SSA [m ² /g]	Band gap energy [eV]
TiO ₂	8.4	169	3.20
10Fe-TiO ₂	8.3	171	3.12
50Fe-TiO ₂	7.9	179	2.90
100Fe-TiO ₂	7.9	179	2.63

153

154

155

156

157

The calculated crystalline size for undoped TiO₂ was 8.4 nm and only a slight decrease for Fe doped TiO₂ samples was observed. Possibly, this phenomenon is due to the entrance of Fe³⁺ into the TiO₂ lattice [23], inducing also an increase of SSA values (Table 2) with respect to undoped TiO₂, as observed in literature [24].

158

159

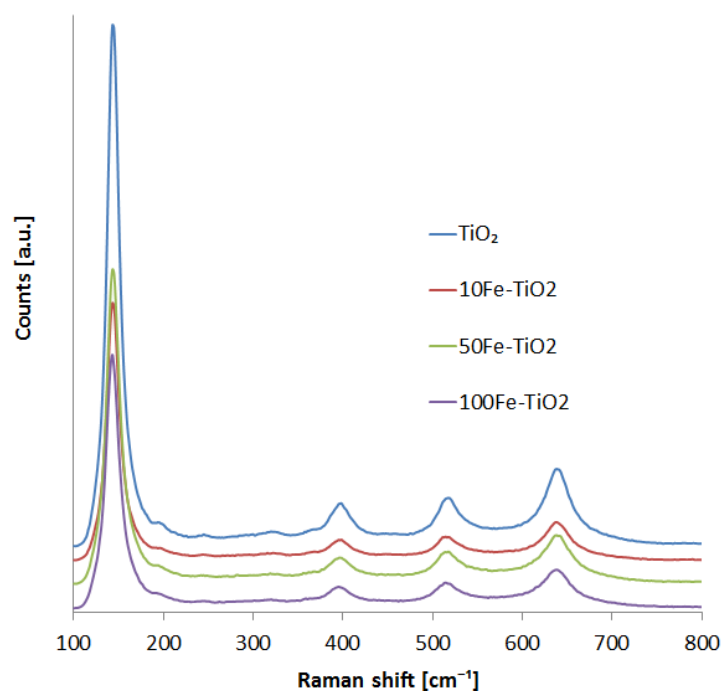
160

161

162

163

Raman spectra in the range of 200-800 cm⁻¹ of the doped catalysts and undoped TiO₂ are shown in Figure 4. In particular, only the TiO₂ common signals at 144, 396, 514, 637 cm⁻¹ and a weak shoulder at 195 cm⁻¹ due to the anatase crystalline phase of TiO₂ are evident [25]. Also in this case, no signals due to iron oxides are evident. These results confirm that TiO₂ doping process was correctly finalized.



164

165

166

Figure 4. Raman spectra of undoped and Fe doped TiO₂ photocatalysts in the range 100–800 cm⁻¹.

167

168

169

Additionally, the intensity of the Raman bands for all the doped samples is lower than those ones of undoped TiO₂, supporting again the incorporation of Fe³⁺ into the substitution site of the TiO₂ lattice [26].

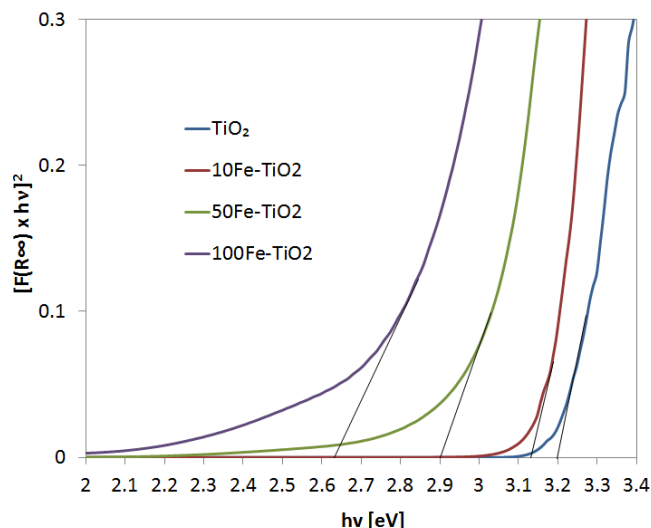
170

171

172

173

The data obtained from UV-Vis reflectance spectra were used for evaluating the band-gap energy of TiO₂ and of Fe-doped TiO₂ photocatalysts (Figure 5). The doping of TiO₂ with iron significantly influenced the band-gap energy value. In fact, as the Fe amount was increased, a decrease of band-gap energy (from 3.20 for undoped TiO₂ to 2.63 eV for 100Fe-TiO₂) was observed.

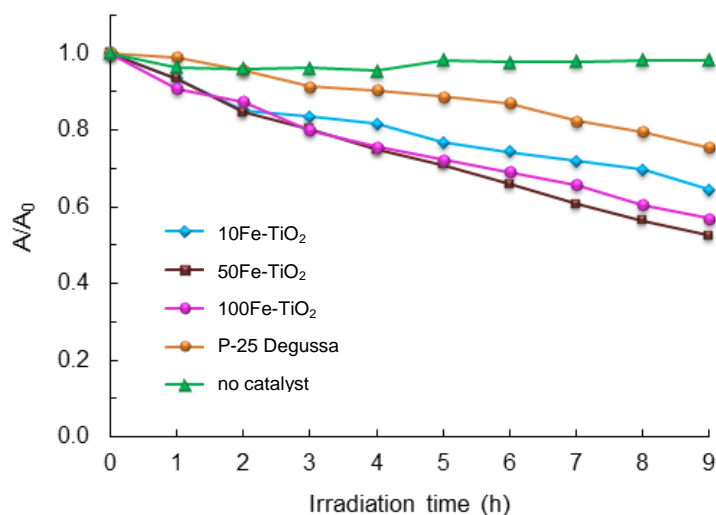


174
175
176 **Figure 5.** Band gap evaluation of for undoped and Fe-doped TiO₂ photocatalysts.

177 This decrease was due to the electronic transition from donor levels formed with dopants to the
178 conduction band of the host photocatalyst [27]. The band-gap energy value of Fe-doped TiO₂
179 samples is an indication of their potential photoactivity under visible light irradiation.

180 3.2. Catalyst Screening and Selection

181 Preliminary experiments were performed to evaluate whether RV5 could be degraded by a
182 photocatalytic treatment. In these experiments, the concentrations of the dye and the catalyst were
183 held constant at 30 ppm and 3 g/L, respectively, so as to operate with a dye-to-catalyst weight ratio
184 of 1:100. The photodegradation process was carried out at the spontaneous pH of the dye solution
185 (pH 7.2) for an overall duration of 10 h (1-h darkness and 9-h irradiation). The following catalysts
186 were tested: P-25 Degussa (P-25) and Fe-doped TiO₂ at three Fe levels: 10Fe-TiO₂, 50Fe-TiO₂ and
187 100Fe-TiO₂. The results are shown in Figure 6.
188



189
190 **Figure 6.** Photocatalytic degradation of Reactive Violet 5 (RV5) in the absence and presence of different
191 catalysts ($c_{RV5}^0 = 30$ ppm; pH = 7.2; catalyst load = 3 g/L). A is the absorbance of the dye solution at 560 nm.

192 The first point to note is that in the absence of catalyst no significant variations in dye
193 concentration were observed, while all catalysts were able to degrade RV5. The removal efficiencies
194 at the end of the treatment ranged from about 23% (P25) to 47.6% (50Fe-TiO₂). Furthermore, a closer
195 analysis of the results in Figure 5 reveals that:

196

197

198

199

200

201

202

203

204

205

206

207

208

- P-25 resulted in a color removal close to 23% at the end of the treatment;
- 100Fe-TiO₂ showed a final decolorization degree close to 42%;
- 10Fe-TiO₂ exhibited an intermediate behavior and decolorized the dye solution to about 35%;
- 50Fe-TiO₂ was the most effective catalyst, with a color removal efficiency of 47.6%.

It may be interesting to consider that, although the band-gap energy of 100Fe-TiO₂ is smaller than that of 50Fe-TiO₂ (2.63 and 2.90 eV, respectively), the first catalyst exhibited a lower photocatalytic activity. This could be due to the higher content of Fe(III) ions, which can act as recombination centers for the photogenerated hole-electron pairs [28,29].

Since 50Fe-TiO₂ was the most effective of the catalysts tested, it was selected as the best catalyst for RV5 degradation under visible light irradiation.

209

3.3. Analysis of the UV-vis Absorption Spectrum of RV5 During Degradation

210

211

212

213

214

215

216

217

218

219

220

221

222

223

224

225

226

227

228

229

230

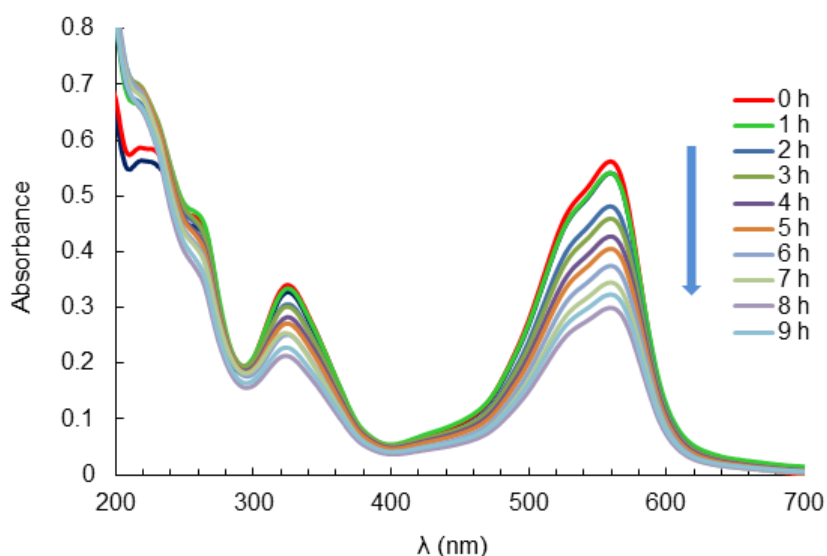
231

232

233

234

235



236

Figure 7. Absorption spectrum of Reactive Violet 5 (RV5) during the photocatalytic treatment.

237

238

239

Therefore, it can be concluded that the photocatalytic treatment of RV5 by the 50Fe-TiO₂ catalyst is effective not only for color removal but also for the degradation of the aromatic structures of the dye molecule and its cleavage into smaller fragments.

240

3.4. Effect of pH

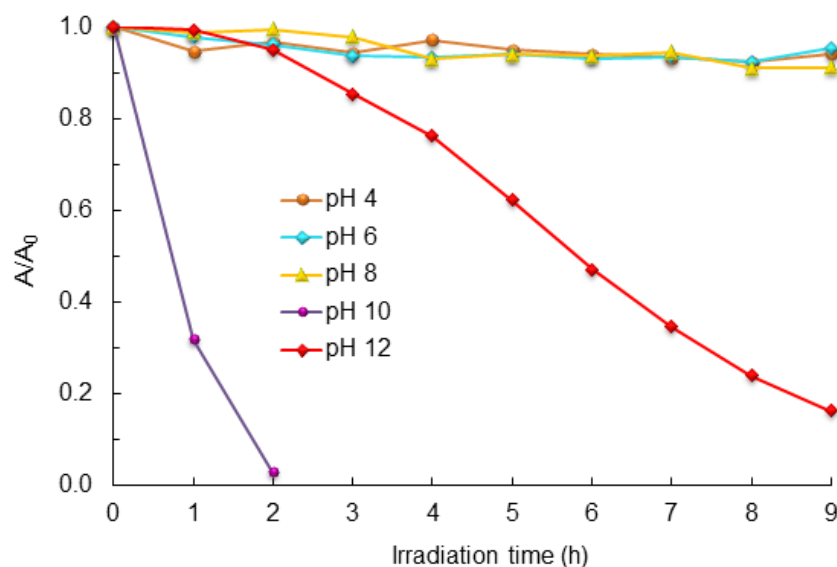
241

242

243

As it is known, pH is one of the most important process parameters for the photocatalytic degradation of dyes [31]. In order to find the optimal pH for RV5 degradation, this parameter was varied from 4 to 12. The initial dye concentration was set at 30 ppm and the catalyst load was 3 g/L.

244 The results obtained during a 10-h treatment period (1-h darkness and 9-h irradiation) are shown in
 245 Figure 8. It can be seen that at lower pH values ($4 \leq \text{pH} \leq 8$) the absorbance at 560 nm remained
 246 almost constant. By contrast, at pH 10 it decreased quickly, reaching a value close to zero after 2-h
 247 irradiation. At pH 12, an intermediate behavior was observed, with the initial absorbance being
 248 halved in about 6 h and reduced by around 80% at the end of the treatment. Thus, it can be
 249 concluded that, under the experimental conditions employed, the optimal pH for RV5 degradation
 250 was equal to 10. Accordingly, further experiments were carried out at this pH.



269 **Figure 8.** Photocatalytic degradation of Reactive Violet 5 (RV5) at different pH values ($c_{\text{RV5}}^0 = 30$ ppm; catalyst
 270 load = 3 g/L). A is the absorbance of the dye solution at 560 nm.

271 The influence of pH on dye removal can be attributed to its effects on the generation of radical
 272 species, particularly hydroxyl radicals ($\cdot\text{OH}$), during the photocatalytic process. These radicals are
 273 produced at the catalyst surface from the oxidation of OH^- or H_2O by the photogenerated holes (h^+):



274 Hydroxyl radicals are powerful oxidizing agents and can easily attack the azo groups in the dye
 275 molecule, breaking the $-\text{N}=\text{N}-$ bonds and causing a decolorization of the dye solution. They can also
 276 attack the aromatic structures of the dye, but these structures are more resistant than azo bonds, so
 277 that decolorization is achieved more easily than degradation [32].

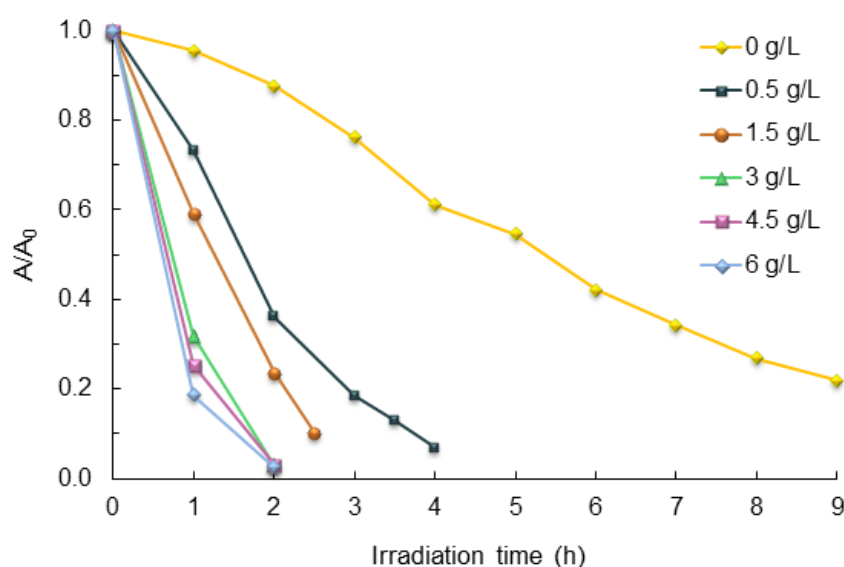
278 From Equations (1) and (2) it can be seen that the production of $\cdot\text{OH}$ is favored under alkaline
 279 conditions, consistently with the results in Figure 8. The enhanced removal of azo dyes at alkaline
 280 pH was observed in several other studies. For example, after 40 min of the photocatalytic treatment
 281 with TiO_2 of a solution containing Reactive Orange 4, the color removal was 25.3% at pH 1 and 90.5%
 282 at pH 9 [33]. The degradation of the dye was less effective, as after 80-min irradiation it passed from
 283 15.2%, at pH 1, to 87.2%, at pH 9. Similar results were obtained in a study on the photocatalytic
 284 degradation of Reactive Black 5 by TiO_2 [34].

285 In addition to the direct effect of pH on the production of $\cdot\text{OH}$ described by Equations (1) and
 286 (2), it should also be considered that [31,35]: (a) the extent of dye adsorption and photon absorption
 287 are also affected by pH; (b) at low pH, H^+ ions can interact with the azo bonds decreasing their
 288 electron density and their susceptibility to electrophilic attack by hydroxyl radicals; and (c) under
 289 acidic conditions, TiO_2 particles tend to agglomerate, reducing the surface area of the catalyst.

290 The observed decrease in color removal at pH 12 could be due to a decreased adsorption of dye
 291 molecules on the catalyst surface. In fact, at this pH the catalyst surface is highly hydroxylated and
 292 hence negatively charged, repelling the RV5 molecules that have charges of the same sign.

293 3.5. Effect of Catalyst Load

294 The amount of catalyst to be used in the photocatalytic treatment is another important factor for
 295 the degradation of pollutants [31]. To evaluate the optimal catalyst load, this quantity was varied
 296 from 0 to 6 g/L, keeping the pH at 10 and the initial dye concentration at 30 ppm. The results of these
 297 experiments are shown in Figure 9. In the absence of catalyst, the decolorization of the dye solution
 298 proceeded quite slowly, with over 20% of the initial amount of RV5 still present at the end of the
 299 treatment. When the catalyst was added at 0.5 g/L, the decolorization was more rapid and completed
 300 in about 4 h. With a catalyst load of 1.5 g/L, this time was reduced to about 3 h. At higher catalyst
 301 loads (3 to 6 g/L), about 2 h were sufficient to achieve complete color removal. Furthermore, the
 302 observed decay curves were very similar to each other.



317
 318 **Figure 9.** Photocatalytic degradation of Reactive Violet 5 (RV5) at different catalyst loads ($c_{RV5}^0 = 30$ ppm;
 319 pH = 10). A is the absorbance the dye solution at 560 nm.

320 A simple kinetic analysis was used to provide a quantitative description of the effect of catalyst
 321 load on dye removal. In particular, the apparent rates of the photocatalytic process were determined
 322 by applying the initial rate method.

323 The initial rate of dye removal ($-r_0$), which is rigorously defined as:

$$-r_0 = - \left. \frac{d(A/A_0)}{dt} \right|_{t=0} \quad (3)$$

324 was calculated as:

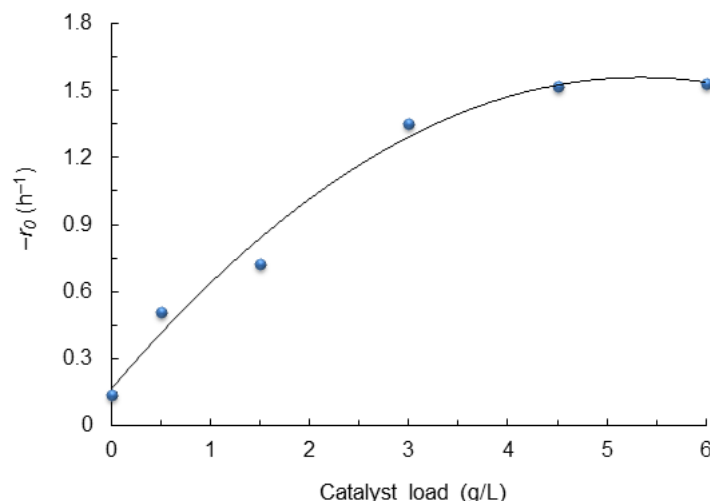
$$-r_0 = - \frac{(A/A_0)_{t_1} - (A/A_0)_{t_0}}{t_1 - t_0} \quad (4)$$

325 with $t_0 = 0$ and $t_1 = 1$ h. In the above equations, A_0 is the absorbance of the dye solution at 560 nm and
 326 at the beginning of irradiation ($t = 0$), while A is the absorbance at time t .

327 From the results in Figure 10 it can be seen that, at catalyst loads lower than 3 g/L, there was a
 328 nearly linear increase of the decolorization rate with the amount of catalyst, while above this value
 329 the effect was very small. Accordingly, a value of 3 g/L was selected as the optimal catalyst load.

330

331
332
333
334
335
336
337
338
339
340
341
342
343
344



345 **Figure 10.** Initial rate of Reactive Violet 5 (RV5) removal as a function of catalyst load ($c_{RV5}^0 = 30$ ppm; pH = 10).

346 The existence of a threshold value for catalyst load has been reported in many studies on the
347 photocatalytic degradation of azo dyes including, for example, Reactive Black 5 [34], Reactive Blue 4
348 [36], Reactive Orange 4 [37], Reactive Red 120 [38], Reactive Blue 19 [39], Reactive Blue 198 and
349 Reactive Yellow 145 [40]. This behavior is likely the result of multiple factors [30]. At low loadings,
350 an increase in the amount of catalyst in the reaction mixture has a positive effect on the kinetics of
351 dye removal due to the increased surface area available for dye adsorption and degradation.
352 However, when all dye molecules are adsorbed on the catalyst surface, further additions of catalyst
353 are no longer effective for decolorization of the dye solution. Moreover, an excessive amount of
354 catalyst can reduce light penetration in the solution due to shielding and scattering effects resulting
355 from aggregate formation. Finally, activated catalyst particles can interact with ground-state
356 particles causing partial deactivation of the catalyst.

357 3.6. Effect of Hydrogen Peroxide

358 The presence of hydrogen peroxide in the reaction medium is known to enhance the rate of
359 photocatalytic degradation of organic compounds [30]. To investigate the effect of hydrogen
360 peroxide on the decolorization of RV5, experiments were performed by adding 10 to 100 mM
361 hydrogen peroxide to a solution at pH 10 containing 30 ppm of dye and 3 g/L of catalyst. The results
362 are presented in Figure 11. As it can be seen, the color removal efficiency increased upon addition of
363 hydrogen peroxide, but the observed decolorization profiles varied not-monotonically with the
364 amount of hydrogen peroxide present in the reaction medium. This can be better appreciated from
365 Figure 12, where the initial rates of dye removal, calculated from Equation (4), are plotted against the
366 initial hydrogen peroxide concentrations. These data reveal that an optimal hydrogen peroxide
367 concentration of 60 mM exists. Similar results were found in other studies on the photocatalytic
368 decolorization of azo dyes under visible light irradiation [34,37,39,41,42].

369 To provide an explanation to the above observation, it should be considered that hydrogen
370 peroxide is an effective electron acceptor and can produce hydroxyl radicals through the following
371 reaction:



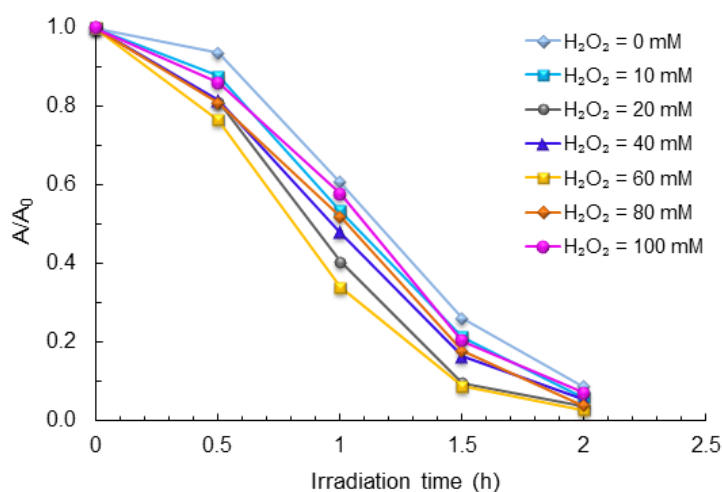
373 Additional hydroxyl radicals can be formed from the reaction of hydrogen peroxide with the
superoxide radical:



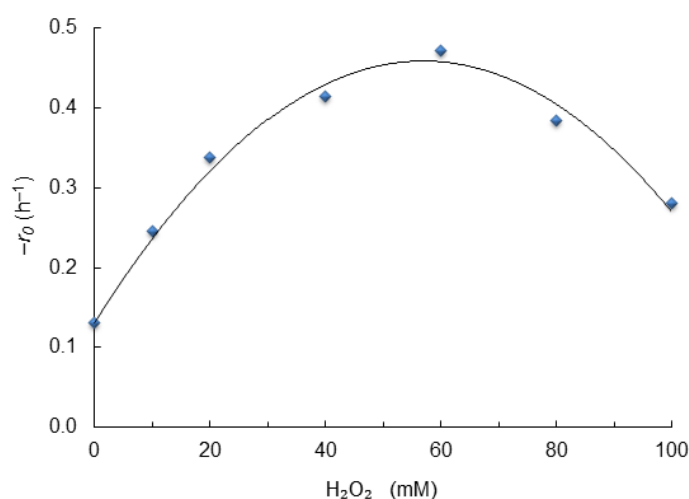
375 However, at high concentrations, hydrogen peroxide can act as a scavenger of hydroxyl
radicals, according to the following reactions [35]:



376 Furthermore, it can also react with TiO_2 to form peroxy compounds that are detrimental to the
 377 degradation process [43]. When the positive and negative effects balance each other, an optimum
 378 will be found for the amount of hydrogen peroxide in the reaction medium.
 379



395 **Figure 11.** Photocatalytic degradation of Reactive Violet 5 (RV5) at different hydrogen peroxide concentrations
 396 ($c^0_{\text{RV5}} = 30$ ppm; pH = 10; catalyst load = 3 g/L). A is the absorbance the dye solution at 560 nm.



413 **Figure 12.** Initial rate of Reactive Violet 5 (RV5) removal as a function of hydrogen peroxide
 414 concentration ($c^0_{\text{RV5}} = 30$ ppm; pH = 10; catalyst load = 3 g/L).

415 3.7. Comparison with the Results of Other Published Studies

416 It may be interesting to compare the present results with those obtained in other studies on the
 417 degradation of RV5.

418 Chung et Chen [12] investigated the photocatalytic degradation of RV5 using TiO₂
419 nanoparticles under UV irradiation. Under optimized conditions, the photodegradation efficiency
420 was 90% after 20 min of irradiation and reached nearly 100% after 80 min.

421 Cabansag et al. [13] studied the degradation of RV5 under UV light with bulk zinc oxide slurry
422 as the photocatalyst. Under optimized conditions, the dye was degraded by 74% after 30 min of
423 irradiation and almost completely after 90 min.

424 Kunal et al. [14] used an acclimatized indigenous bacterial mixed culture isolated from a dye
425 contaminated soil to degrade RV5. The mixed culture was composed of six bacterial strains
426 including *Bacillus*, *Lysinibacillus* and *Ochrobacterium* species and was grown in a minimal medium
427 containing glucose and yeast extract. Under static growth conditions at 37 °C and pH 7, the dye
428 solution was completely decolorized in about 18 h. However, in the absence of carbon and nitrogen
429 sources only about 4% of the initial amount of dye was degraded after the same time, indicating that
430 these sources are essential for the treatment.

431 Bheemaraddi et al. [15] investigated the ability of a bacterial strain of *Paracoccus* sp. isolated
432 from a textile mill effluent to degrade RV5 as the sole source of carbon. Under static conditions and
433 with minimal nutritional requirements this strain allowed complete decolorization of the dye
434 solution within 16 h.

435 Finally, Ayed et al. [16] explored the feasibility of using a consortium of *Staphylococcus* species,
436 two of which were isolated from a textile wastewater, to degrade RV5. Under optimal conditions,
437 the dye solution was completely (>99%) decolorized within 8 h. The decolorization was also
438 accompanied by a high COD removal (94.93%)

439 Therefore, the results obtained in the present study indicate that the degradation of RV5 by a
440 Fe-doped titania catalyst under visible light irradiation can lead to dye removal efficiencies that are
441 comparable with those reported for UV-photocatalytic or microbial treatments. Moreover, compared
442 to microbial degradation processes, the investigated technology is simpler to implement and more
443 flexible in operation.

444 4. Conclusions

445 The presence of dyes in industrial effluents is an issue of major concern due to the detrimental
446 effects that these pollutants could have on the environment. In this study we have shown that RV5,
447 an azo dye widely used in the textile industry, can be effectively degraded by a photocatalytic
448 treatment using a Fe-doped TiO₂ catalyst under visible light irradiation. An analysis of the effects of
449 the main process parameters (pH, catalyst load and hydrogen peroxide concentration) on the dye
450 removal efficiency showed that the process can be optimized to provide rapid and complete
451 degradation. The use of visible light and the relatively short treatment times support the suitability
452 of the proposed process as a promising and cost-effective method for the removal of this or similar
453 dyes from textile effluents.

454 Future studies should be directed at investigating the effects of the treatment on dye
455 mineralization and evaluating the optimal conditions for mineralization. The identification of
456 reaction products and intermediates formed during the treatment could be helpful to elucidate the
457 mechanisms involved in RV5 degradation.

458 **Author Contributions:** Conceptualization, Antonio Zuurro; Investigation, Marika Michela Monaco;
459 Methodology, Antonio Zuurro, Roberto Lavecchia, Giuseppina Iervolino and Vincenzo Vaiano; Supervision,
460 Antonio Zuurro; Writing – original draft, Antonio Zuurro and Giuseppina Iervolino; Writing – review &
461 editing, Roberto Lavecchia and Marika Michela Monaco.

462 **Funding:** This research was partially supported by grants from Sapienza University of Rome (Italy).

463 **Conflicts of Interest:** The authors declare no conflict of interest.

464 References

465 1. Hunger, K. *Industrial Dyes: Chemistry, Properties, Applications*; Wiley-VCH: Weinheim, Germany, 2003.

- 466 2. Clark, M. Handbook of Textile and Industrial Dyeing – Volume 1: Principles, Processes and Types of Dyes;
467 Woodhead Publishing: Cambridge, UK, 2011; pp. 428–438.
- 468 3. Zuorro, A.; Maffei, G.; Lavecchia, R. Kinetic modeling of azo dye adsorption on non-living cells of
469 *Nannochloropsis oceanica*. *J. Environ. Chem. Eng.* **2017**, *5*, 4121–4127.
- 470 4. Petrucci, E.; Di Palma, L.; Lavecchia, R.; Zuorro, A. Treatment of diazo dye Reactive Green 19 by anodic
471 oxidation on a boron-doped diamond electrode. *J. Ind. Eng. Chem.* **2015**, *26*, 116–121.
- 472 5. Yaseen, D.A.; Scholz, M. Textile dye wastewater characteristics and constituents of synthetic effluents: A
473 critical review. *Int. J. Environ. Sci. Technol.* **2019**, *16*, 1193–1226.
- 474 6. Ventura-Camargo, B.C.; Marin-Morales, M.A. Azo dyes: Characterization and toxicity – A review. *Text.*
475 *Light Ind. Sci. Technol.* **2013**, *2*, 85–103.
- 476 7. Chung, K.-T. Azo dyes and human health: A review. *J. Environ. Sci. Health Pt. C-Environ. Carcinog.*
477 *Ecotoxicol. Rev.* **2016**, *34*, 233–261.
- 478 8. Parvathi, C.; Maruthavanan, T.; Sivamani, S.; Prakash, C. Removal of dyes from textile wet processing
479 industry: A review. *J. Text. Assoc.* **2011**, *71*, 319–323.
- 480 9. Singh, K.; Arora, S. Removal of synthetic textile dyes from wastewaters: A critical review on present
481 treatment technologies. *Crit. Rev. Environ. Sci. Technol.* **2011**, *41*, 807–878.
- 482 10. Vogelpohl, A.; Kim, S.M. Advanced oxidation processes AOPs in wastewater treatment. *J. Ind. Eng. Chem.*
483 **2004**, *10*, 33–40.
- 484 11. Oturan, M.A.; Aaron, J.-J. Advanced oxidation processes in water/wastewater treatment: Principles and
485 applications. A review. *Crit. Rev. Environ. Sci. Technol.* **2014**, *44*, 2577–2641.
- 486 12. Chung, Y.C.; Chen, C.Y. Degradation of azo dye reactive violet 5 by TiO₂ photocatalysis. *Environ. Chem.*
487 *Lett.* **2009**, *7*, 347–352.
- 488 13. Cabansag, J.L.J.; Dumelod, J.C., Alfaro, J.C.O.; Arsenal, J.D.; Sambot, J.C.; Enerva, L.T.; Leañó Jr, J.L.
489 Photocatalytic degradation of aqueous C.I. Reactive Violet 5 using bulk zinc oxide (ZnO) slurry. *Philipp. J.*
490 *Sci.* **2013**, *142*, 77–85.
- 491 14. Kunal, J.; Varun, S.; Digantkumar, C.; Datta, M. Decolorization and degradation of azo dye – Reactive
492 Violet 5R by an acclimatized indigenous bacterial mixed cultures-SB4 isolated from anthropogenic dye
493 contaminated soil. *J. Hazard. Mat.* **2012**, *213-214*, 378–386.
- 494 15. Bheemaraddi, M.C.; Patil, S.; Shivannavar, C.T.; Gaddad, S.M. Isolation and characterization of *Paracoccus*
495 *sp.* GSM2 capable of degrading textile azo dye Reactive Violet 5. *Sci. World J.* **2014**, *2014*, 410704.
- 496 16. Ayed, L.; Bekir, K.; Achour, S.; Cheref, A.; Bakhrouf, A. Exploring bioaugmentation strategies for azo
497 dye CI Reactive Violet 5 decolourization using bacterial mixture: Dye response surface methodology.
498 *Water Environ. J.* **2017**, *31*, 80–89.
- 499 17. Iervolino, G.; Vaiano, V.; Rizzo, L. Visible light active Fe-doped TiO₂ for the oxidation of arsenite to
500 arsenate in drinking water. *Chem. Eng. Trans.* **2018**, *70*, 1573–1578.
- 501 18. Vaiano, V.; Iervolino, G.; Sannino, D.; Rizzo, L.; Sarno, G. MoO_x/TiO₂ immobilized on quartz support as
502 structured catalyst for the photocatalytic oxidation of As(III) to As(V) in aqueous solutions, *Chem. Eng. Res.*
503 *Des.* **2016**, *109*, 190–199.
- 504 19. Pongwan, P.; Inceesungvorn, B.; Wetchakun, K.; Phanichphant, S.; Wetchakun, N. Highly efficient
505 visible-light-induced photocatalytic activity of Fe-doped TiO₂ nanoparticles. *Eng. J.* **2012**, *16(3)*, 143–151.
- 506 20. Li, Z.; Shen, W.; He, W.; Zu, X. Effect of Fe-doped TiO₂ nanoparticle derived from modified hydrothermal
507 process on the photocatalytic degradation performance on methylene blue. *J. Hazard. Mater.* **2008**, *155*, 590–
508 594.
- 509 21. Sun, L.; Zhai, J.; Li, H.; Zhao, Y.; Yang, H.; Yu, H. Study of homologous elements: Fe, Co, and Ni dopant
510 effects on the photoreactivity of TiO₂ nanosheets. *ChemCatChem* **2014**, *6*, 339–347.
- 511 22. Yang, Y.; Yu, Y.; Wang, J.; Zheng, W.; Cao, Y. Doping and transformation mechanisms of Fe³⁺ ions in
512 Fe-doped TiO₂. *CrystEngComm* **2017**, *19*, 1100–1105.
- 513 23. Marami, M.B.; Farahmandjou, M.; Khoshnevisan, B. Sol-gel synthesis of Fe-doped TiO₂ nanocrystals. *J.*
514 *Electron. Mater.* **2018**, *47*, 3741–3748.
- 515 24. Zhou, M.; Yu, J.; Cheng, B. Effects of Fe-doping on the photocatalytic activity of mesoporous TiO₂ powders
516 prepared by an ultrasonic method. *J. Hazard. Mater.* **2006**, *137*, 1838–1847.
- 517 25. Gao, Y.; Luan, T.; Lü, T.; Cheng, K.; Xu, H. Performance of V₂O₅-WO₃-MoO₃/TiO₂ catalyst for selective
518 catalytic reduction of NO_x by NH₃, *Chin. J. Chem. Eng.* **2013**, *21*, 1–7.

- 519 26. Prajapati, B.; Kumar, S.; Kumar, M.; Chatterjee, S.; Ghosh, A.K. Investigation of the physical properties of
520 Fe:TiO₂-diluted magnetic semiconductor nanoparticles. *J. Mater. Chem. C* **2017**, *5*, 425–4267.
- 521 27. Wang, W.; Tadó, M.O.; Shao, Z, Research progress of perovskite materials in photocatalysis and
522 photovoltaics-related energy conversion and environmental treatment, *Chem. Soc. Rev.*, **2015**, *44*, 5371–
523 5408.
- 524 28. Navio, J.A.; Testa, J.J.; Djedjeian, P.; Padron, J.R.; Rodriguez, D. Iron-doped titania powders prepared by a
525 sol-gel method. Part II: Photocatalytic properties. *Appl. Catal. A-Gen.* **1999**, *178*, 191–203.
- 526 29. Serpone, N.; Lawless, D.; Disdier, D. Spectroscopic, photoconductivity, and photocatalytic studies of TiO₂
527 colloids: Naked and with the lattice doped with Cr³⁺, Fe³⁺, and V⁵⁺ cations. *Langmuir* **1994**, *10*, 643–652.
- 528 30. Petrucci, E.; Di Palma, L.; Lavecchia, R.; Zuurro, A. Modeling and optimization of Reactive Green 19
529 oxidation on a BDD thin-film electrode. *J. Taiwan Inst. Chem. Eng.* **2015**, *51*, 152–158.
- 530 31. Ajmal, A.; Majeed, I.; Malik, R.N.; Idriss, H.; Nadeem, M.A. Principles and mechanisms of photocatalytic
531 dye degradation on TiO₂ based photocatalysts: A comparative overview. *RSC Adv.* **2014**, *4*, 37003–37026.
- 532 32. Wu, C.H. Photodegradation of C.I. Reactive Red 2 in UV/TiO₂-based systems: Effects of ultrasound
533 irradiation. *J. Hazard. Mat.* **2009**, *167*, 434–439.
- 534 33. Muruganandham, M.; Swaminathan, M. Solar photocatalytic degradation of a reactive azo dye in
535 TiO₂-suspension. *Sol. Energy Mater. Sol. Cells* **2004**, *81*, 439–457.
- 536 34. Muruganandham, M.; Sobana, N.; Swaminathan, M. Solar assisted photocatalytic and photochemical
537 degradation of Reactive Black 5. *J. Hazard. Mater.* **2006**, *137*, 1371–1376.
- 538 35. Fox, M.A.; Dulay, M.T. Heterogeneous photocatalysis. *Chem. Rev.* **1993**, *93*, 341–357.
- 539 36. Samsudin, E.M.; Goh, S.N.; Wu, T.Y.; Ling, T.T.; Hamid, S.B.A.; Juan, J.C. Evaluation on the photocatalytic
540 degradation activity of Reactive Blue 4 using pure anatase nano-TiO₂. *Sains Malays.* **2015**, *44*, 1011–1019.
- 541 37. Gonçalves, M.S.T.; Pinto, E.M.S.; Nkeonye, P.; Oliveira-Campos, A.M.F. Degradation of C.I. Reactive
542 Orange 4 and its simulated dyebath wastewater by heterogeneous photocatalysis. *Dyes Pigment.* **2005**, *64*,
543 135–139.
- 544 38. Kavitha, S.K.K.; Palanisamy, P.N. Photocatalytic and sonophotocatalytic degradation of Reactive Red 120
545 using dye sensitized TiO₂ under visible light. *World Acad. Sci. Eng. Technol.* **2011**, *73*, 1–6.
- 546 39. Saquib, M.; Muneer, M. Semiconductor mediated photocatalysed degradation of an anthraquinone dye,
547 Remazol Brilliant Blue R under sunlight and artificial light source. *Dyes Pigment.* **2002**, *53*, 237–249.
- 548 40. Thamaraiselvi, K.; Sivakumar, T. Photocatalytic activities of novel SrTiO₃-BiOBr heterojunction catalysts
549 towards the degradation of reactive dyes. *Appl. Catal. B-Environ.* **2017**, *207*, 218–232.
- 550 41. Neppolian, B., Choi H. C., Sakthivel S., Arabindoo B., Murugesan, V. (2002). Solar light induced and TiO₂
551 assisted degradation of textile dye reactive blue 4. *Chemosphere*, *46*, 1173–1181.
- 552 42. Thi Dung, N.; Van Khoa, N.; Herrmann, J.M. Photocatalytic degradation of reactive dye RED-3BA in
553 aqueous TiO₂ suspension under UV-visible light. *Int. J. Photoenergy* **2005**, *7*, 11–15.
- 554 43. Poullos, I.; Tsachpinis, I. Photodegradation of the textile dye Reactive Black 5 in the presence of
555 semiconducting oxides. *J. Chem. Technol. Biotechnol.* **1999**, *74*, 349–357.